Journal of the Oceanographical Society of Japan
Vol. 34, pp. 117 to 128, 1978

A Model on the Turbulent Wind Field over Wind-waves in Curvilinear Co-ordinates*

Hiroshi ICHIKAWA**

Abstract: The wave-induced fluctuations of wind velocity over wind-waves measured in the wind tunnel experiment (ICHIKAWA and IMASATO, 1976) are compared with the numerical results estimated by a linear model (Model II) on the turbulent wind field over a dominant component of wind-waves. In the Model II, the undulation of mean air flow is introduced by adopting the curvilinear co-ordinates, and the existence of viscous sublayer and the influence of underlying wind-waves to background atmospheric turbulence are taken into account. The numerical results estimated by the Model II are in good agreement with the experimental results. The good agreement, which was not obtained from the previous model (Model I) in the Cartesian co-ordinates, is shown to be attributed to the undulating mean flow introduced in the Model II.

1. Introduction

In order to understand the mechanism of momentum and energy-transfers from wind to wave, it is necessary to clarify the structure of wind field over wind-waves. BARNETT and KENYON (1975) concluded that the earlier theoretical models which did not account for the existence of atmospheric turbulence have been unable to explain the actual wind field over wind-waves. ICHIKAWA and IMASATO (1976) reaffirmed that the vertical changes of the wave-induced fluctuations of wind velocities and the wave-induced Reynolds stress over wind-waves are different from those predicted by the Miles' (1957) quasi-laminar model. They compared their experimental results with the numerical results estimated by a model (hereafter refered to be as Model I) on the turbulent wind field over wind-waves and confirmed again that the discrepancy may be attributed to the existence of atmospheric turbulence neglected by MILES (1957). In the Model I, the wind field is formulated in the Cartesian co-ordinates and the boundary conditions are given at the mean water surface level assuming the infinitesimal wave.

* Received Feb. 20, revised July 24 and accepted Sept. 11, 1978.

** Geophysical Institute, Faculty of Science, Kyoto University, Kitashirakawa Oiwake-cho, Sakyo-ku, Kyoto 606, Japan

However, the Model I was not necessarily appropriate to predict the wind field over wind-waves. Actually, it could not predict the phase difference of wind velocities in respect to the underlying dominant component wave. The critical layer, which plays an important role in the energy transfer from wind to waves, is undulated by the corrugation of wavy boundary surface. In many cases of wind tunnel experiment, this undulating critical layer crosses the mean water surface level because the mean height of the undulating critical layer is lower than the wave-crests. Therefore, in the case of wind tunnel experiment, it is not appropriate to give the boundary conditions at the mean water surface level assuming the infinitesimal wave. The discrepancy in the previous paper of ICHIKAWA and IMASATO (1976) may be attributed to the facts that the undulation of mean air flow was not taken into account and that the boundary conditions were not given at the wavy water surface.

In order to overcome these weak points, the adoption of the curvilinear orthogonal system of co-ordinates is the most natural way, *i.e.*, in the curvilinear co-ordinates (ξ, η) proposed by BENJAMIN (1959), the boundary conditions can be given just at the wavy boundary surface and the undulating critical layer can be easily represented by an undulating line of a constant value of η. MILES (1959) and BENJAMIN (1959)

have already discussed the wind field over wavy water surface by the use of the curvilinear co-ordinates. However, neither of them took into account the existence of the atmospheric turbulence. Recently, using the curvilinear co-ordinates, GENT and TAYLOR (1976) proposed a nonlinear numerical model on the deep turbulent wind field over a wavy water surface. However, the viscous sublayer neglected by them will exist when the wind speed is fairly small (IMASATO, 1976). GENT and TAYLOR (1976) showed that the predicted fractional rate of energy input from wind to waves for the uniform surface roughness is of the same order of magnitude as in Miles' (1957, 1959) and Townsend's (1972) linear theories. This result suggests that the contribution from nonlinearity of wind field to the predicted wind field is not large. They showed also that the variation of surface roughness caused by the short waves riding on the wavy surface significantly increases the fractional rate of energy input. However, the variable surface roughness in their model is rather arbitrary. Therefore, another linear model (hereafter refered to be as Model II) on the turbulent wind field over a dominant component of wind-waves in the wind tunnel is proposed in this paper, using the curvilinear co-ordinates. In the Model II, the existence of viscous sublayer neglected by GENT and TAYLOR (1976) is taken into account when the wind speed is fairly small and a parameter representing the rate of increase of eddy viscosity due to underlying wind-waves is introduced, conjecturing that the fluctuation of wind velocity induced by underlying wind-waves will increase the energy of background atmospheric tubulence over wind-waves as proposed by GENT and TAYLOR (1976).

In this paper, the previous results in the wind tunnel experiment (ICHIKAWA and IMASATO, 1976) will be compared with the numerical results estimated by the Model II.

2. Theoretical model

2.1. *System of co-ordinates and govering equation*

We consider the turbulent wind field in a frame of reference travelling in positive x_1-direction with the phase velocity C of a dominant component wave of wind-waves. The

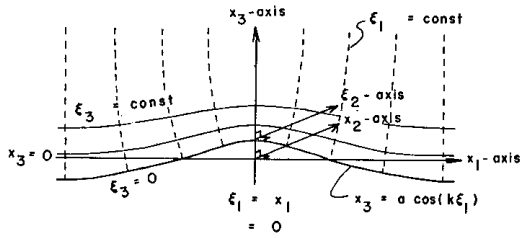

Fig. 1. Curvilinear orthogonal system of co-ordinates (ξ_1, ξ_2, ξ_3) and Cartesian system of co-ordinates (x_1, x_2, x_3).

Cartesian system of co-ordinates (x_1, x_2, x_3) is illustrated in Fig. 1. The surface displacement ζ of the component wave in the reference frame is represented by

$$\zeta = a \cos(kx_1) \tag{2.1}$$

where a is the wave-amplitude and k the wave-number of the dominant wave. It is assumed in this paper that $(ak)^2$ is negligibly small, the wind field is homogeneous in the x_2-direction and that the mean horizontal wind velocity $U(x_3)-C$ in the reference frame has only the component parallel to x_1-axis.

In the formulation of wind field over the dominant wave, we adopt the curvilinear co-ordinates (ξ_1, ξ_2, ξ_3) illustrated in Fig. 1. In this co-ordinates system, the Cartesian system of co-ordinates (x_1, x_2, x_3) is expressed as follows,

$$\begin{cases} x_1 = \xi_1 - a \exp(-k\xi_3) \sin(k\xi_1) \\ x_2 = \xi_2 \\ x_3 = \xi_3 + a \exp(-k\xi_3) \cos(k\xi_1) \end{cases}$$

The curvilinear system of co-ordinates adopted in this paper is essentially as same as those adopted by BENJAMIN (1959) and GENT and TAYLOR (1976). The Jacobian J of this transformation, correct to the order of ak, is represented by

$$J = \partial(\xi_1, \xi_2, \xi_3)/\partial(x_1, x_2, x_3) = 1 + 2\,ak \exp(-k\xi_3) \cos(k\xi_1)$$

The undulating line of $\xi_3 = 0$ is expressed in the Cartesian co-ordinates by

$$x_3 = a \cos(k\xi_1)$$

which equals the water surface displacement ζ in Eq. (2.1) to the order of ak. Therefore, the wind field in the region between a wave-crest and a wave-trough can be treated in this curvi-

linear co-ordinates although it can not be treated in the Cartesian co-ordinates assuming the infinitesimal wave. It must be mentioned here that this curvilinear co-ordinates can be well defined only over a monochromatic wave. The adoption of this co-ordinates system in the formulation of wind field over the random wavy surface can only be qualitative. If the power spectrum of wind-waves has a fairly narrow peak and the crests of wind-waves are observed to be fairly long, the adoption of this curvilinear co-ordinates will be useful to formulate the turbulent wind field over a dominant component of wind-waves.

Hereafter, all variables and co-ordinates will be expressed in non-dimensional form, taking k^{-1} and C as the scales of the length and the velocity, respectively.

The wind velocity $\boldsymbol{u}$ in the turbulent wind field in the reference frame is decomposed into the undisturbed part $\bar{\boldsymbol{u}}$, the wave-induced periodic part $\tilde{\boldsymbol{u}}$ and the random background turbulence $\boldsymbol{u}^t$, *i.e.*,

$$\boldsymbol{u}=\bar{\boldsymbol{u}}(\xi_3)+\tilde{\boldsymbol{u}}(\xi_1,\xi_3)+\boldsymbol{u}^t(\xi_1,\xi_2,\xi_3,t) \quad (2.2)$$

where t is the time. The time average at fixed points in the reference frame, denoted by the operator $\langle\ \rangle$, of $\boldsymbol{u}^t$ is vanished and the time average of $\boldsymbol{u}$ is represented by

$$\langle\boldsymbol{u}\rangle=\bar{\boldsymbol{u}}(\xi_3)+\tilde{\boldsymbol{u}}(\xi_1,\xi_3)$$

The non-dimensional mean wind velocity $\bar{u}_1(\xi_3)$ parallel to ξ_1-axis has not been clarified yet, and it is assumed to be equal to the mean horizontal wind velocity at the height $x_3=\xi_3$, *i.e.*,

$$\bar{\boldsymbol{u}}(\xi_3)=(U(\xi_3)-1,0,0) \quad (2.3)$$

Owing to this treatment, the mean flow undulation caused by the corrugation of wavy boundary surface can be easily introduced in the analysis as a mean flow parallel to undulating line of constant ξ_3.

We define the stream function ϕ representing the time averaged velocity components as follows,

$$\langle u_1(\xi_1,\xi_3)\rangle=J^{1/2}\frac{\partial}{\partial\xi_3}\phi(\xi_1,\xi_3)$$

$$\langle u_3(\xi_1,\xi_3)\rangle=-J^{1/2}\frac{\partial}{\partial\xi_1}\phi(\xi_1,\xi_3)$$

where u_n is the ξ_n-component of wind velocity. ϕ is decomposed into the undisturbed part $\bar{\phi}$ and the wave-induced periodic part $\tilde{\phi}$, *i.e.*,

$$\phi(\xi_1,\xi_3)=\bar{\phi}(\xi_3)+\tilde{\phi}(\xi_1,\xi_3)$$

$\bar{\phi}(\xi_3)$ is defined by

$$\bar{\phi}(\xi_3)=\int_0^{\xi_3}\bar{u}_1(\xi_3)d\xi_3$$

$\tilde{\phi}(\xi_1,\xi_3)$ is considered to be expressed by

$$\tilde{\phi}(\xi_1,\xi_3)=a\Re\mathfrak{e}\{\hat{\phi}(\xi_3)\exp(j\xi_1)\}$$

where $\Re\mathfrak{e}$ indicates the real part of a complex variable, $\hat{\phi}$ the complex amplitude of $\tilde{\phi}$ and $j=\sqrt{-1}$. From the definition of ϕ, the wave-induced periodic parts of the ξ_1 and ξ_3-components of wind velocity, correct to the order of a, are represented as follows, respectively,

$$\tilde{u}_1(\xi_1,\xi_3)=a\bar{u}_1(\xi_3)\exp(-\xi_3)\cos(\xi_1)+a\Re\mathfrak{e}\{\hat{\phi}'(\xi_3)\exp(j\xi_1)\} \quad (2.4)$$

$$\tilde{u}_3(\xi_1,\xi_3)=a\Re\mathfrak{e}\{-j\hat{\phi}(\xi_3)\exp(j\xi_1)\} \quad (2.5)$$

where prime denotes the differentiation on ξ_3. The first term in the right-hand side of Eq. (2.4) originates from the periodic part of the Jacobian J and it represents the contribution from undulating mean flow to $\tilde{u}_1$.

The turbulent Reynolds stress r_{nm} denoted by

$$r_{nm}=\langle-u^t{}_n\,u^t{}_m\rangle$$

is assumed to be decomposed into the mean part $\bar{r}_{nm}$ and the wave-induced periodic part $\tilde{r}_{nm}$, *i.e.*,

$$r_{nm}=\bar{r}_{nm}(\xi_3)+\tilde{r}_{nm}(\xi_1,\xi_3) \quad (2.6)$$

$\tilde{r}_{nm}$ is assumed to be represented by

$$\tilde{r}_{nm}(\xi_1,\xi_3)=a\Re\mathfrak{e}\{\hat{r}_{nm}(\xi_3)\exp(j\xi_1)\}$$

taking the first term of Fourier series expansion of $\tilde{r}_{nm}$. Here, $\hat{r}_{nm}$ is the complex amplitude of $\tilde{r}_{nm}$.

The equation of motion is expressed in vector form as follows,

$$\frac{\partial}{\partial t}\boldsymbol{u}+\mathrm{grad}\left(\frac{1}{2}\boldsymbol{u}\cdot\boldsymbol{u}\right)-\boldsymbol{u}\times\mathrm{rot}\,\boldsymbol{u}=-\frac{1}{\rho_a}\mathrm{grad}\,p+\nu_a(\mathrm{grad.\ div}\,\boldsymbol{u}-\mathrm{rot.\ rot}\,\boldsymbol{u}) \quad (2.7)$$

where p is the static pressure, ρ_a the density of air and ν_a the kinematic molecular viscosity of air. Eliminating the pressure term, the vorticity equation in vector form is derived as follows,

$$\frac{\partial}{\partial t}\mathrm{rot}\,\boldsymbol{u}-\mathrm{rot}\,(\boldsymbol{u}\times\mathrm{rot}\,\boldsymbol{u}) =-\nu_a\ \mathrm{rot.\ rot.\ rot}\,\boldsymbol{u} \qquad (2.8)$$

Substituting Eq. (2.2) into Eq. (2.8) and taking the time average, the time averaged vorticity equation in the reference frame is derived as follows,

$$-\mathrm{rot}\,(\bar{\boldsymbol{u}}\times\mathrm{rot}\,\bar{\boldsymbol{u}}+\tilde{\boldsymbol{u}}\times\mathrm{rot}\,\bar{\boldsymbol{u}}+\bar{\boldsymbol{u}}\times\mathrm{rot}\,\tilde{\boldsymbol{u}}) =-\nu_a\ \mathrm{rot.\ rot.\ rot}\,(\bar{\boldsymbol{u}}+\tilde{\boldsymbol{u}})+\boldsymbol{T}+\boldsymbol{W} \qquad (2.9)$$

where $\boldsymbol{T}$ is the contribution from $\boldsymbol{u}^t$ and $\boldsymbol{W}$ the contribution from $\tilde{\boldsymbol{u}}$. $\boldsymbol{T}$ and $\boldsymbol{W}$ are denoted by Eqs. (2.10) and (2.11), respectively,

$$\boldsymbol{T}=\langle\mathrm{rot}\,(\boldsymbol{u}^t\times\mathrm{rot}\,\boldsymbol{u}^t)\rangle \qquad (2.10)$$

$$\boldsymbol{W}=\langle\mathrm{rot}\,(\tilde{\boldsymbol{u}}\times\mathrm{rot}\,\tilde{\boldsymbol{u}})\rangle \qquad (2.11)$$

Using the equation of continuity about $\boldsymbol{u}^t$ and Eq. (2.6), the ξ_2-component T_2 of $\boldsymbol{T}$, which is correct to the order of a, can be represented by

$$T_2=\bar{r}_{13}''+a\exp(-\xi_3)\Re\mathfrak{e}[\{2(\bar{r}_{13}''+\bar{r}_{13}'-2\bar{r}_{13}) +j(\bar{r}_{33}'-\bar{r}_{11}'-2\bar{r}_{33}+2\bar{r}_{11})\}\exp(j\xi_1)] +a\Re\mathfrak{e}[\{\hat{r}_{13}''+\hat{r}_{13}+j(\hat{r}_{11}'-\hat{r}_{33}')\}\exp(j\xi_1)] \qquad (2.12)$$

The second term in the right-hand side of Eq. (2.12) originates from the periodic part of J. In order to solve Eq. (2.9) on $\tilde{\boldsymbol{u}}$, the turbulent Reynolds stresses have to be related to $\bar{\boldsymbol{u}}$ and $\tilde{\boldsymbol{u}}$.

The overall average of the ξ_1-component of Eq. (2.7), which is correct to the order of a, is represented by

$$\bar{r}_{13}'(\xi_3)+\nu_a\bar{u}_1''(\xi_3)=0$$

Then, the mean tangential turbulent Reynolds stress $\bar{r}_{13}$ is represented by

$$\bar{r}_{13}(\xi_3)=u_*^2-\nu_a\bar{u}_1'(\xi_3) \qquad (2.13)$$

where u_* is the friction velocity of air. The eddy viscosity ν_s associated with the vertical shear of mean wind velocity satisfies the following relation,

$$\bar{r}_{13}(\xi_3)=2\nu_s(\xi_3)\,\bar{e}_{13}(\xi_3) =\nu_s(\xi_3)\bar{u}_1'(\xi_3) \qquad (2.14)$$

where $\bar{e}_{13}\,(=1/2\,\bar{u}_1')$ is the undisturbed part of the tangential rate-of-strain e_{13}. From Eqs. (2.13) and (2.14), ν_s is represented by

$$\nu_s(\xi_3)=u_*^2/\bar{u}_1'(\xi_3)-\nu_a \qquad (2.15)$$

It is noticed in Eq. (2.13) that the dependency of the mean tangential turbulent Reynolds stress over the wavy surface to ξ_3 is as same as that over the flat wall boundary to the distance from the wall boundary surface. Therefore, refering to the experimental results on the pipe flow (HINZE, 1959, Figs. 7-34 and 7-38), it is assumed that the mean normal turbulent Reynolds stresses over wavy surface are represented as follows, respectively,

$$\bar{r}_{11}(\xi_3)=-5.8\bar{r}_{13}(\xi_3) \qquad (2.16)$$

$$\bar{r}_{33}(\xi_3)=-0.6\bar{r}_{13}(\xi_3) \qquad (2.17)$$

The wave-induced variations $\tilde{r}_{nm}$ of turbulent Reynolds stresses are assumed to have the same form as in the Yefimov's (1970) model, *i.e.*,

$$\tilde{r}_{11}=\tilde{r}_{33} \qquad (2.18)$$

$$\tilde{r}_{13}=2\nu_e\tilde{e}_{13} =2\nu_e a\Re\mathfrak{e}\{\hat{e}_{13}(\xi_3)\exp(j\xi_1)\} \qquad (2.19)$$

where $\hat{e}_{13}$ is the complex amplitude of the wave-induced periodic part $\tilde{e}_{13}$ of tangential rate-of-strain and ν_e is the eddy viscosity relating $\tilde{r}_{13}$ to $\tilde{e}_{13}$. In the curvilinear co-ordinates, $\hat{e}_{13}$ is expressed by

$$\hat{e}_{13}(\xi_3)=\frac{1}{2}[\hat{\phi}''(\xi_3)+\hat{\phi}(\xi_3) +2\exp(-\xi_3)\{\bar{u}_1'(\xi_3)-\bar{u}_1(\xi_3)\}] \qquad (2.20)$$

The third term in the brackets [ ] originates from the periodic part of J and it represents the contribution from undulating mean flow to $\tilde{e}_{13}$.

Although ν_e is assumed to have an arbitrary constant value in the Yefimov's model, it will be vanished in the viscous sublayer where the turbulent fluctuation of wind velocity does not exist. DAVIS (1972) and REYNOLDS and HUSSAIN (1972) proposed a theoretical model in which ν_e is always equal to ν_s. However, it is

difficult to consider that ν_e relating $\tilde{r}_{13}$ to $\tilde{e}_{13}$ is always equal to ν_s which satisfies Eq. (2.14). It can be conjectured, as was proposed by GENT and TAYLOR (1976), that the fluctuations of wind velocity induced by underlying wind-waves will increase the energy of background atmospheric turbulence over wind-waves. It is assumed in this paper that ν_e is α times ν_s, *i.e.*,

$$\nu_e(\xi_3)=\alpha\cdot\nu_s(\xi_3) \tag{2.21}$$

where α is a non-dimensional parameter with a positive constant value representing the rate of increase of eddy viscosity due to underlying wind-waves. The numerical solutions are obtained for arbitrary values of α from 0.5 to 20.

Substituting Eqs. (2.18) and (2.19) into Eq. (2.12), the wave-induced periodic part of ξ_2-component of vorticity equation (2.9), which is correct to the order of a, can be derived as follows,

$$\begin{aligned}\bar{u}_1(\hat{\phi}''-\hat{\phi})-\hat{\phi}\bar{u}_1''=&-j\nu_a(\hat{\phi}''''-2\hat{\phi}''+\hat{\phi})\\&-j\nu_e(\hat{\phi}''''+2\hat{\phi}''+\hat{\phi})-2j\nu_e'(\hat{\phi}'''+\hat{\phi}')\\&-j\nu_e''(\hat{\phi}''+\hat{\phi})+A\end{aligned} \tag{2.22}$$

where

$$\begin{aligned}A=&\{(\bar{r}_{33}'-\bar{r}_{11}')-2(\bar{r}_{33}-\bar{r}_{11})-2j(\bar{r}_{13}'-2\bar{r}_{13})\}\\&\times\exp(-\xi_3)-2[\bar{u}_1'\bar{u}_1+j\{\nu_a(\bar{u}_1'''-2\bar{u}_1'')\\&+\nu_e(\bar{u}_1'''-3\bar{u}_1''+4\bar{u}_1'-2\bar{u}_1)+2\nu_e'(\bar{u}_1''-2\bar{u}_1'\\&+\bar{u}_1)+\nu_e''(\bar{u}_1'-\bar{u}_1)\}]\exp(-\xi_3)\end{aligned} \tag{2.23}$$

and $\boldsymbol{W}$ in Eq. (2.9) is neglected because the magnitude of wave-induced Reynolds stress is the order of a^2. From Eqs. (2.4), (2.12) and (2.20), it can be said that the term A originates from the periodic part of the Jacobian J, and that the second term in the right-hand side of Eq. (2.23) represents the contribution from undulating mean flow to periodic part of vorticity equation.

2.2. Boundary conditions

The ξ_3-component $\langle u_3(\xi_1,0)\rangle$ of wind velocity at the wavy water surface $\xi_3=0$ must be vanished because the wavy water surface is stationary in the reference frame. From Eqs. (2.3) and (2.5), this condition is represented by

$$\hat{\phi}(0)=0 \tag{2.24}$$

The tangential component $\langle u_1(\xi_1,0)\rangle$ at the wavy surface satisfies the condition of non-slipping relative to the water particle just at the wavy water surface, *i.e.*,

$$\begin{aligned}\langle u_1(\xi_1,0)\rangle&=\bar{u}_1(0)+\tilde{u}_1(\xi_1,0)\\&=\langle u_c(\xi_1)\rangle\end{aligned}$$

where u_c is the tangential velocity of water at the wavy surface. $\langle u_c\rangle$ is considered to be represented in dimensional form as follows

$$\langle u_c(\xi_1)\rangle=\bar{u}_c-C+kC\zeta(\xi_1)+\tilde{u}_{\mathrm{rot}}(\xi_1)$$

where $\bar{u}_c$ is the mean tangential velocity of water, $kC\zeta$ the tangential component of orbital velocity of wave at $\xi_3=0$, which is correct to the order of a, and $\tilde{u}_{\mathrm{rot}}$ the periodic part of the tangential component of rotational velocity of water. We assume that $\bar{u}_c$ is negligibly small compared with the phase velocity of the dominant component wave. Then, the non-dimensional mean wind velocity $\bar{u}_1(0)$ is represented by

$$\bar{u}_1(0)=-1$$

The wind-wave can be considered to be fairly irrotational. It is assumed that $\tilde{u}_{\mathrm{rot}}$ is negligibly small compared with $kC\zeta$. Then, using Eq. (2.4), the following condition is derived,

$$\hat{\phi}'(0)=2 \tag{2.25}$$

The wave-induced periodic fluctuations of wind velocity at $\xi_3=H$ are vanished and this requires that

$$\hat{\phi}(H)=0 \tag{2.26}$$

$$\hat{\phi}'(H)=-\bar{u}_1(H)\exp(-H) \tag{2.27}$$

where H is the height sufficiently far from the wavy surface.

2.3. Mean wind profile

It is well known that the vertical profile of mean horizontal wind velocity $U(x_3)$ in the turbulent boundary layer higher than the wave-crests is logarithmic with respect to x_3. On the other hand, $U(x_3)$ in the region between wave-crests and wave-troughs can not be measured directly. It is assumed, as was proposed by DAVIS (1972), that the vertical profile of $U(x_3)$ is linear with respect to x_3 in the layer (named as "linear sublayer" in this paper) of which thickness z_1 equals $z_0\exp(\Delta U)$ where z_0 is the roughness height and ΔU the thickness

parameter of "linear sublayer". We assume that the non-dimensional mean wind velocity $\bar{u}_1(\xi_3)$ parallel to ξ_1-axis is represented as follows,

$$\bar{u}_1(\xi_3)=U(\xi_3)-1$$
$$\begin{cases}\dfrac{u_*}{\kappa}\ln(\xi_3/z_0)-1, & \xi_3\geqq z_1\\ \dfrac{u_*}{\kappa}G(\Delta U)\xi_3/z_0-1, & \xi_3\leqq z_1\end{cases} \tag{2.28}$$

using Eq. (2.3). Here, κ is the Kármán constant and $G(\Delta U)\equiv\Delta U\exp(-\Delta U)$.

If we assume that the eddy viscosity ν_s defined by Eq. (2.15) is not negative in the "linear sublayer", ΔU satisfies the following relation,

$$\kappa u_* z_0/G(\Delta U)-\nu_a\geqq 0 \tag{2.29}$$

The function $G(\Delta U)$ has the maximum value of $\exp(-1)$ at $\Delta U=1$. Therefore, when the parameter $D\equiv\kappa u_* z_0/\nu_a$ is smaller than $G(1)$, ΔU has the minimum value of ΔU_m which satisfies the relation (2.29). The "linear sublayer" for $\Delta U=\Delta U_m$ is coincident with the viscous sublayer and in that sublayer ν_s vanishes. Neglecting the existence of viscous sublayer, GENT and TAYLOR (1976) assumed that the "initial" vertical profile of mean wind velocity is represented by

$$\bar{u}_1(\xi_3)=\frac{u_*}{\kappa}\ln\left(\frac{\xi_3+z_0}{z_0}\right)-1 \tag{2.30}$$

However, the viscous sublayer will exist when the wind speed is fairly small. The numerical solutions are obtained for $\Delta U=\Delta U_m$ when the parameter D is smaller than $G(1)$. On the other hand, when the parameter D is greater than $G(1)$, ΔU can be arbitrary positive. In this case, the numerical solutions are obtained for arbitrary values of ΔU from unity to ten.

The finite differential equation derived from Eq. (2.22) is integrated numerically with the boundary conditions (2.24)~(2.27). The finite difference length $\Delta\xi_3$ and the upper limit H of the integration are chosen to be 0.001 and 4.0, respectively. The numerical solution estimated for $\Delta\xi_3=0.0005$ and $H=6.0$ is nearly equal to that estimated for $\Delta\xi_3=0.001$ and $H=4.0$.

3. Result and discussion

3.1. Numerical results

In the wind tunnel experiment performed by ICHIKAWA and IMASATO (1976), the power spectrum of wind-waves had a fairly narrow peak and the crests of the wind-waves seemed fairly long. The numerical solutions estimated by the present model Model II are compared with the experimental results of ICHIKAWA and IMASATO (1976) in quantities $\sigma_u^2, \sigma_w^2, \theta_u, \theta_w$ and τ at the frequency of the wave spectral peak, which are the non-dimensional powers of the wave-induced fluctuations of horizontal and vertical wind velocities, the phase-difference of the wave-induced fluctuations of horizontal and vertical wind velocities in respect to a component wave of underlying wind-waves and the non-dimensional wave-induced Reynolds stress, respectively. They are expressed as follows,

$$\sigma_u^2(x_3)=\frac{1}{2}|\hat{v}_1(x_3)|^2 \tag{3.1}$$

$$\sigma_w^2(x_3)=\frac{1}{2}|\hat{v}_3(x_3)|^2 \tag{3.2}$$

$$\theta_u(x_3)=\tan^{-1}[-\hat{v}_{1i}(x_3)/+\hat{v}_{1r}(x_3)] \tag{3.3}$$

$$\theta_w(x_3)=\tan^{-1}[-\hat{v}_{3i}(x_3)/\hat{v}_{3r}(x_3)] \tag{3.4}$$

$$\tau(x_3)=\frac{-1}{2}\{\hat{v}_{1r}(x_3)\hat{v}_{3r}(x_3)+\hat{v}_{1i}(x_3)\hat{v}_{3i}(x_3)\} \tag{3.5}$$

where suffixes r and i denote the real and imaginary parts of the complex amplitude $\hat{v}_n(x_3)$ of the wave-induced fluctuation $\tilde{v}_n$ of wind velocity parallel to x_n-axis, respectively. $\tilde{v}_n$ is represented by

$$\tilde{v}_n(x_1, x_3)=a\Re\{\hat{v}_n(x_3)\exp(jx_1)\}$$

It must be noticed that $\hat{v}_1$ and $\hat{v}_3$ are defined at a constant height from the mean water surface level, but that the stream function $\hat{\phi}$ is defined along the undulating line of a constant value of ξ_3. Owing to the relation between the Cartesian system and the curvilinear system, $\hat{v}_1$ and $\hat{v}_3$ are related to $\hat{\phi}(\xi_3)$, which satisfies Eq. (2.22) at $\xi_3=x_3$, as follows, respectively,

$$\hat{v}_1(x_3)=\hat{\phi}'(\xi_3)$$
$$-\exp(-x_3)\{U'(x_3)-U(x_3)+1\} \tag{3.6}$$

$$j\cdot\hat{v}_3(x_3)=\hat{\phi}(\xi_3)$$
$$-\exp(-x_3)\{U(x_3)-1\} \tag{3.7}$$

which are correct to the order of a. Each

second term in the right-hand side of Eqs. (3.6) and (3.7) represents the contribution from mean flow undulation caused by the corrugation of wavy boundary to the wave-induced fluctuations of horizontal and vertical wind velocities.

In order to examine the calculated wind fields in different conditions of mean wind velocity and of dominant component wave, the numerical solutions are obtained for the experimental cases of Run-I, II and III (ICHIKAWA and IMASATO, 1976). The parameters of the vertical profile of mean wind velocity and the wind-wave field in each experimental case are tabulated in Table 1. u_* and z_0 are the known values from the experiment, but the parameters α and ΔU are chosen so that the numerical solutions agree with the experimental results.

Figs. 2, 3 and 4 show the measured and calculated vertical profiles of σ_u^2, σ_w^2, θ_u, θ_w and τ in the cases of Run-I, II and III, respectively. The numerical solutions in these figures are obtained for some values of α from two to ten. In the cases of Run-I and II, the parameter D is smaller than $G(1)$, and therefore, the existence of viscous sublayer is taken into account. In the case of Run-I, the value of ΔU_m is 7.49, and then, the thickness z_1 of the "linear sublayer" which coincides with the viscous sublayer

Table 1. The conditions of the vertical profile of mean wind velocity and the wind-wave field.

		Run-I	Run-II	Run-III
u_*	(cm s^{-1})	9.39	23.0	43.3
z_0	(cm)	0.000167	0.00286	0.0209
f_p	(Hz)	3.60	2.30	1.80
k	(cm^{-1})	0.512	0.212	0.130
Mean amplitude	(cm)	0.132	0.840	1.74
u_*/C		0.212	0.338	0.499

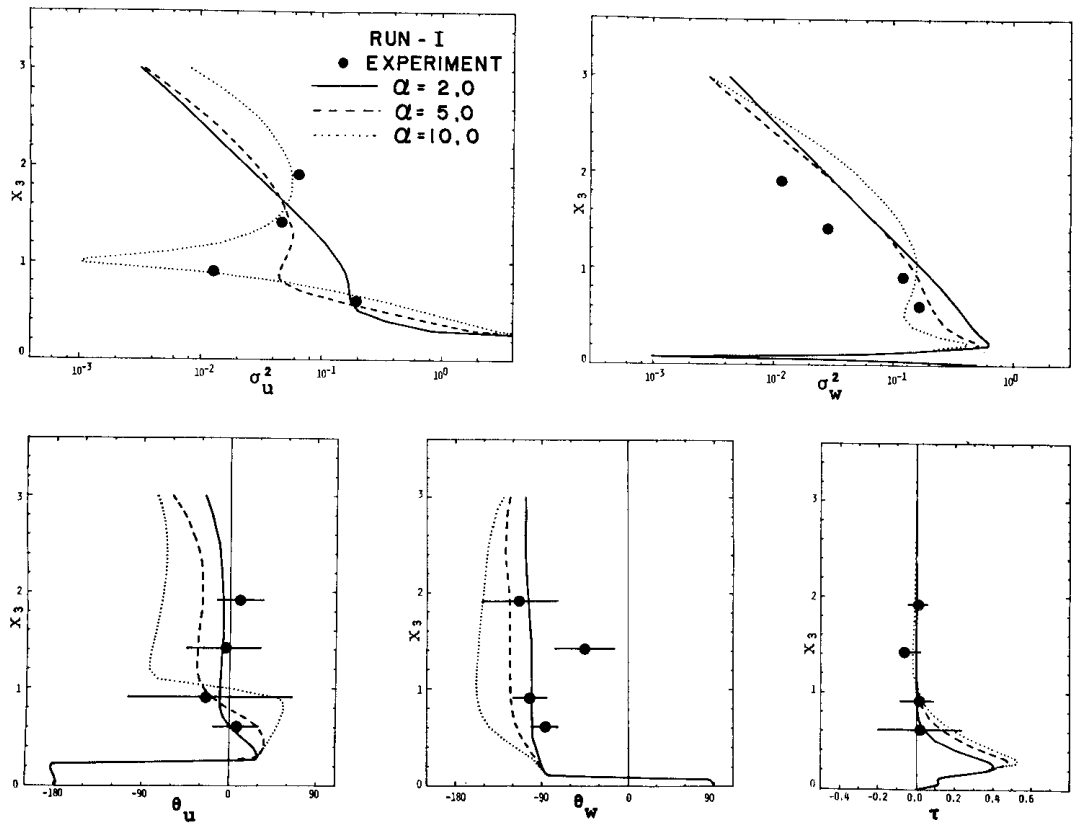

Fig. 2. Vertical profiles of σ_u^2, σ_w^2, θ_u, θ_w and τ obtained from Model II corresponding to the experimental case of Run-I and those of the observed values (mark ●). The variable range of θ_u, θ_w and τ under the 95% confidence limit is shown by the line through the closed circle. x_3 is the height non-dimensionalized by the wave-number. The value of α is in the range from 2.0 to 10.0.

is 0.153. The value of ΔU_m and z_1 in the case of Run-II are 2.25 and 0.006, respectively. On the other hand, in the case of Run-III, the parameter D is greater than $G(1)$, and therefore, ΔU can be arbitrary positive. The numerical solutions for $\Delta U=3.0$ ($z_1=0.055$) are shown in Fig. 4 as an example. It is recognized in these figures that the vertical profiles estimated by the Model II with a suitable value of α have good agreement with the experimental results, especially the vertical profiles of θ_u and θ_w which were not explained well by the previous model of ICHIKAWA and IMASATO (1976).

In Fig. 5 are shown the vertical profiles of σ_u^2 estimated in the case of Run-I for the logarithmic wind profile denoted by Eq. (2.30) and those for $\Delta U=8.0$ ($z_1=0.255$). It is apparent that the numerical solutions for the logarithmic wind profile can not explain the experimental results, and that the numerical solutions for $\Delta U=8.0$ have larger discrepancy from the experimental results than those estimated for $\Delta U=\Delta U_m$. Although it is not shown in any figure, the influence of the existence of "linear sublayer" to the numerical solution is fairly small when the thickness z_1 of "linear layer" is much smaller than unity, and when the parameter D is greater than $G(1)$, the numerical solutions estimated for large z_1 do not agree well with the experimental results. It can be said that the existence of viscous sublayer neglected by GENT and TAYLOR (1976) must be taken into account when the wind speed is fairly small, and that the thickness of the "linear sublayer" must be much smaller than unity when the parameter D is greater than $G(1)$.

The suitable value of α in the cases of Run-II and III are found to be in the range from two to ten. But, it is apparent that the suitable value of α to explain well the measured vertical profile of σ_u^2 in the case of Run-I is in the range from five to ten. This result suggests that the suitable value of α may depends on the underlying wind-wave field and the friction

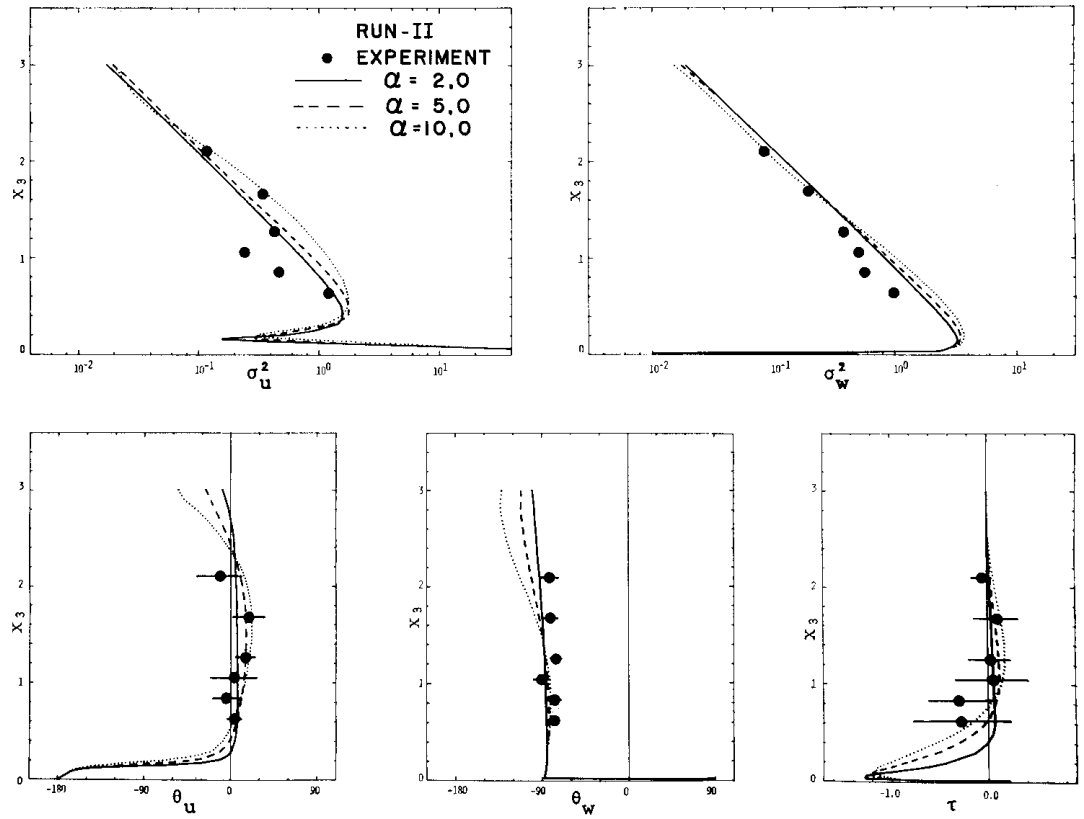

Fig. 3. Vertical profiles of σ_u^2, σ_w^2, θ_u, θ_w and τ calculated from Model II in the experimental case of Run-II and those of the observed values.

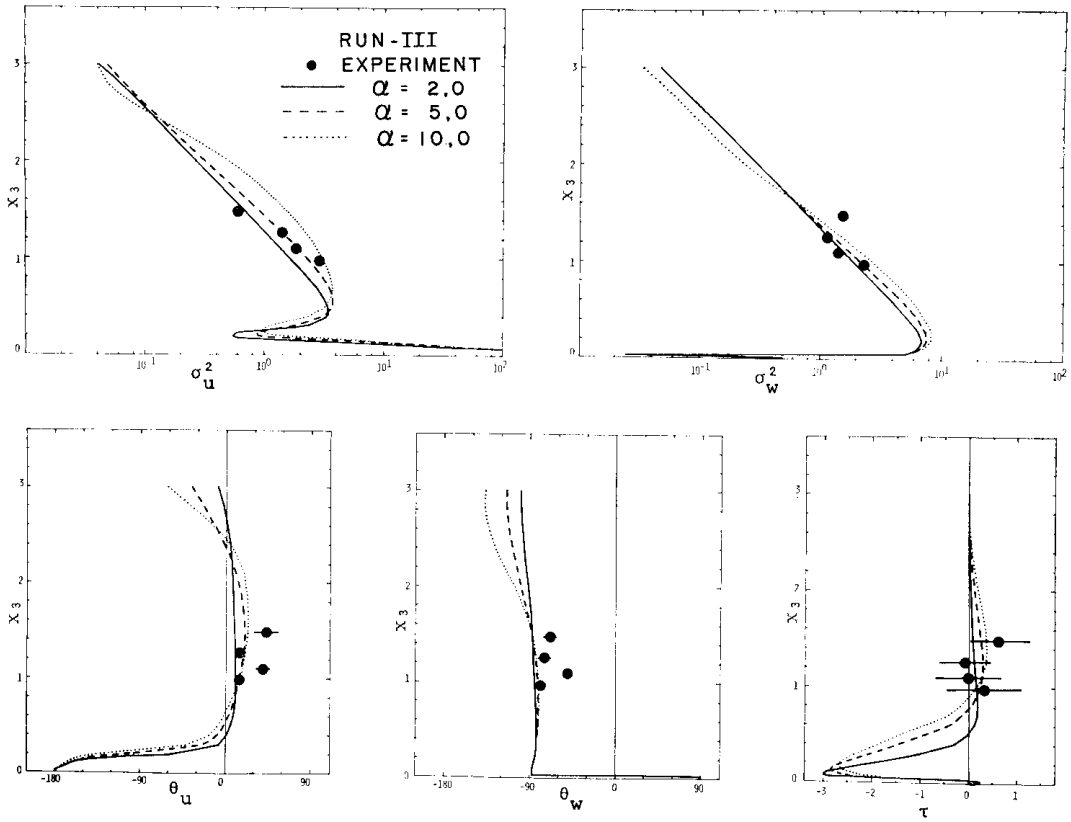

Fig. 4. Vertical profiles of σ_u^2, σ_w^2, θ_u, θ_w and τ calculated from Model II in the experimental case of Run-III and those of the observed values.

velocity of air. A more elaborate discussion on the parameter α will be made in the following paper.

We have assumed rather arbitrarily the wave-induced variations of normal turbulent Reynolds stresses as described in section 2.1. REYNOLDS and HUSSAIN (1972) proposed another model in which $\tilde{r}_{11}$ and $\tilde{r}_{33}$ are related to the wave-induced variation of normal rate-of-strain. $\tilde{r}_{11}$ and $\tilde{r}_{33}$ in their model are rewriten in the curvilinear co-ordinates as follows,

$$\begin{aligned}\tilde{r}_{11}(\xi_1,\xi_3) &= -\tilde{r}_{33}(\xi_1,\xi_3)\\ &= 2\nu_e a\Re\mathrm{e}[\{j\hat{\phi}'(\xi_3)\\ &\quad +\exp(-\xi_3)\bar{u}_1(\xi_3)\}\exp(j\xi_1)] \qquad (3.8)\end{aligned}$$

The numerical solutions estimated by the Model IIa in which $\tilde{r}_{11}$ and $\tilde{r}_{33}$ are given by Eq. (3.8) instead of Eq. (2.18) are nearly equal to those obtained from the Model II. This result suggests that the contributions from $\tilde{r}_{11}$ and $\tilde{r}_{33}$ represented by Eq. (2.18) or (3.8) to the numerical

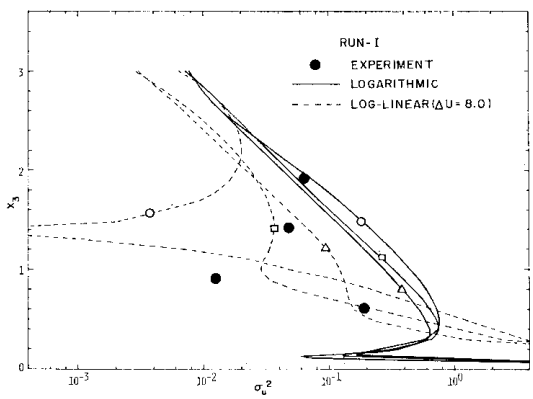

Fig. 5. Vertical profiles of σ_u^2 calculated in the case of Run-I for the logarithmic wind profile, —— and those for $\Delta U=8.0$, - - - -. The value of α is in the range from 2.0 to 10.0 ($\alpha=2.0$, △; $\alpha=5.0$, □; $\alpha=10.0$, ○). ●, experimental results.

solution are much smaller than those from other terms in Eq. (2.22).

3.2. Undulation of mean flow

The Model II differs from our previous Model I not only in the co-ordinates system but also in introducing the mean flow undulation and in the assumptions on the eddy viscosity and on the vertical profile of mean wind velocity in the close visinity of wavy surface. In order to examine the influence of the difference between the assumptions adopted in the Model II and those adopted in the Model I, another numerical model (named as Model IIb) was performed in the curvilinear co-ordinates under the same assumptions as is adopted in the Model I; *i.e.*, the eddy viscosity is constant with reprect to ξ_3 and the value of ΔU is zero.

Figs. 6 and 7 show the measured and calculated vertical profiles of θ_u and θ_w in the case of Run-II, respectively. The calculated vertical profiles in these figures are estimated by the Model I and IIb for the same value (1.5×10^3 $cm^2\,s^{-1}$) of the eddy viscosity. Comparing the solutions estimated by the Model IIb with the solutions in Fig. 3, it can be said that the numerical results obtained from the Model II and those obtained from the Model IIb are qualitatively similar to each other although the numerical solutions estimated by the Model II have better agreement with the experimental results than those estimated by the Model IIb.

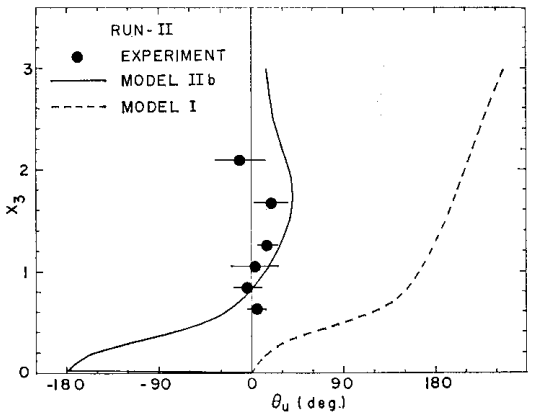

Fig. 6. Vertical profiles of θ_u calculated from Model I and Model IIb in the experimental case of Run-II and those of the observed value. The variable range of θ_u under the 95% confidence limit is shown by the line through the closed circle. The value of ν_e is 1.5×10^3 cm^2s^{-1}.

Further, it is seen in Figs. 6 and 7 that the numerical results obtained from the Model IIb are largely different from those estimated by the Model I in spite of the fact that the assumptions on the eddy viscosity and mean wind profile adopted in the Model IIb are equal to those adopted in the Model I.

The undisturbed part $\bar{\psi}(\xi_3)$ of the non-dimensional stream function, which represents originally the mean flow undulation caused by the corrugation of wavy boundary, is expressed by the Taylor series expansion in the Cartesian co-ordinates as follows,

$$\bar{\psi}(\xi_3)=\phi_1(x_1,x_3)+\frac{1}{2}\bar{u}_1'(x_3)\times\{-a\exp(-x_3)\cos(x_1)\}^2+\frac{1}{6}\bar{u}_1''\{-a\exp(-x_3)\cos(x_1)\}^3+\ldots \quad (3.9)$$

where

$$\phi_1(x_1,x_3)=\bar{\psi}(x_3)-a\bar{u}_1(x_3)\exp(-x_3)\cos(x_1)$$

It must be noticed that only ϕ_1 can be used in a linear theory in the Cartesian co-ordinates to represent the undulating mean flow. However, $\bar{u}_1(x_3)$ vanishes at the critical height $x_3=z_c$ and the stream line of $\phi_1(x_1,x_3)=\bar{\psi}(z_c)$ is parallel to x_1-axis at $x_3=z_c$. Therefore, the undulation of mean flow can not be completely represented by ϕ_1 alone. It can be easily derived that the numerical solution estimated by the linear model Model Ia in the Cartesian co-ordinates, in which

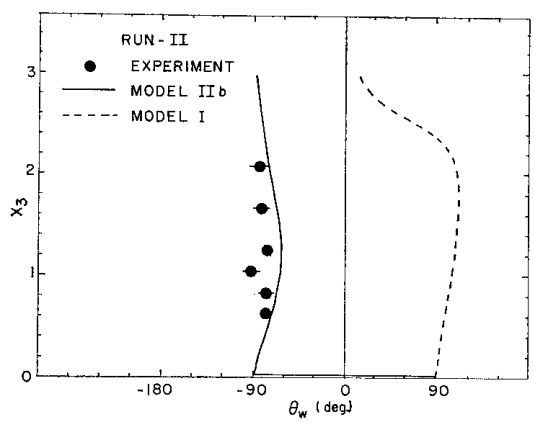

Fig. 7. Vertical profiles of θ_w calculated from Model I and Model IIb in the experimental case of Run-II and those of the observed value.

the undulating mean flow is represented by ϕ_1 alone, coincides with that estimated by the Model I. Therefore, it can be said that the large difference between the numerical results estimated by the Model I and those estimated by the Model IIb originates from the higher order terms than the order of a^2 in the right-hand side of Eq. (3.9) which are originally included in the linear model Model II by the use of $\bar{\phi}(\xi_3)$. It can be concluded that the good agreement between the experimental and numerical results shown in Figs. 2, 3 and 4 is attributed to the fact that not only the existence of atmospheric turbulence but also the undulating mean flow are taken into account in the Model II. Any linear model in the Cartesian co-ordinates will be unable to explain well the wind field over wind-waves in the wind tunnel where the mean height of undulating critical layer is lower than wave-crests. This result suggests that the momentum and energy-transfers from wind to waves must be estimated in the curvilinear co-ordinates when the mean height of undulating critical layer is lower than wave-crests.

It must be mentioned that the Model II can be applied only to the wind field over a dominant component wave of well long-crested wind-waves. In order to clarify the wind field over other component waves and that over random wavy surface, many efforts will have to be made. More detailed measurements of wind field over wind-waves are needed, especially the direct measurements of wind field in the region between the crest and troughs of wind-waves.

Acknowledgements

The author wishes to express his thanks to Prof. H. KUNISHI of Kyoto University for his discussion and encouragement. He also expresses his gratitude to Dr. N. IMASATO of Kyoto University for his gracious disscussion throughout this study. The numerical calculations in this paper were carried out on FACOM 230-75 and FACOM M-190 in the Data Processing Center of Kyoto University.

References

BARNETT, T. P. and K. E. KENYON (1975): Recent advances in the study of wind waves. Rep. Prog. Phys., **38**, 667-729.

BENJAMIN, T. B. (1959): Shearing flow over a wavy boundary. J. Fluid Mech., **6**, 161-205.

DAVIS, R. E. (1972): On the prediction of the turbulent flow over a wavy boundary. J. Fluid Mech., **52**, 287-306.

GENT, P. R. and P. A. TAYLOR (1976): A numerical model of the air flow above water waves. J. Fluid Mech., **77**, 105-128.

HINZE, J. O. (1959): Turbulence. McGraw-Hill Book Co. Inc., New York, 586 pp.

ICHIKAWA, H. and N. IMASATO (1976): The wind field over wind-waves. J. Oceanogr. Soc. Japan, **32**, 271-283.

IMASATO, N. (1976): The mechanism of the development of wind-wave spectra. J. Oceanogr. Soc. Japan, **32**, 253-266.

MILES, J. W. (1957): On the generation of surface waves by shear flows. J. Fluid Mech., **3**, 185-204.

MILES, J. W. (1959): On the generation of surface waves by shear flows. Part 2. J. Fluid Mech., **6**, 568-582.

REYNOLDS, W. C. and A. K. M. F. HUSSAIN (1972): The mechanics of an organized wave in turbulent shear flow. Part 3. Theoretical models and comparisons with experiments. J. Fluid Mech., **54**, 263-288.

TOWNSEND, A. A. (1972): Flow in a deep turbulent boundary layer over a surface distorted by water waves. J. Fluid Mech., **55**, 719-735.

YEFIMOV, V. V. (1970): On the structure of the wind velocity field in the atmospheric near-water layer and the transfer of wind energy to sea waves. Izv. Atmos. Oceanic Phys., **6**, 1043-1058.

風波上の乱れた風の場に関する曲線座標系でのモデル

市　川　　洋*

要旨: 風波の卓越成分波の上の乱れた風の場に関する線型モデル (Model II) の数値解と ICHIKAWA and IMASATO (1976) が風洞水槽実験で得た風波の上の波によって誘起された風速変動との比較を行なった. Model II では曲線座標系の採用によって平均流のうねりを導入し，粘性底層の存在および下の風波の大気乱流への影響を考慮に入れている. Model II の数値解は実験結果とよく一致した. デカルト座標系での以前のモデル (Model I) では得られなかった実験との良い一致は Model II で導入した平均流のうねりによることを示す.

* 京都大学理学部地球物理学教室
〒606 京都市左京区北白川追分町